New Multiband Coupling Matrix Synthesis Technique and Its Microstrip Implementation

Yi-Ting Kuo, Jhe-Ching Lu, Ching-Ku Liao, and Chi-Yang Chang, *Member, IEEE*

***Abstract*—In this paper, we present a novel analytical multiband transversal coupling matrix synthesis technique. By properly combining several single-band filtering functions, the multiband filtering function with flexible transmission zeros and various bandwidth are available. The transversal coupling scheme is then transformed into a practically realizable coupling scheme. To verify the feasibility of the proposed method, two dual-band coupling schemes, both single-path and dual-path, are proposed as examples of the dual-band filter design. Finally, the dual-band filter, based on the coupling matrix corresponding to a specific coupling scheme, can be realized using a microstrip parallel-coupled structure.**

***Index Terms*—Coupling matrix synthesis, multiband filter, microstrip parallel-coupled filter, transmission zeros.**

I. Introduction

RECENT developments in coupling matrix synthesis for single-band filter design is very attractive. Analytical methods for the single-band filter synthesis [1]–[4] are proposed to generate a transversal coupling matrix. For other specific coupling schemes, the coupling matrices are obtained using matrix rotation or optimization [5], [6]. For dual-band or multiband filters, however, a fully analytical solution for transversal coupling matrix synthesis, is still unavailable.

To design dual-band or multiband filters, many methods were proposed. Frequency transformation [7]–[9] was proposed to generate the response function analytically for dual-band filters. It was developed with governing equations of single-band filters. It was unrealizable, however, for multiband filters. Another method was based on parallel-coupled line model [10]; this was used to generate the dual-band performance. This method was limited for dual-band filters, though, and could not be used for multiband filters.

To obtain the multiband performance, an equivalent lumped-element network [11]–[13] was introduced. This network simplified the design procedure for dual-band or multiband filters via the iterative procedure. The problems, however, such as the need for optimization for roots finding [11], [13] or inability to achieve equal ripple [12], occurred while applying those equivalent networks.

In filter design, the coupling matrix technique is well known to have advantages in the hardware implementation. To take advantage of coupling matrices for dual-band or multiband filters, optimization methods [14], [15] were proposed to generate the coupling matrix numerically, via proper cost functions. Fully analytical coupling matrix synthesis for dual-band or multiband filters, however, has not been proposed yet.

In this paper, we propose a novel fully analytical method for the synthesis of multiband transversal coupling matrix. The response function of the multiband filter is generated via the proper combination of single-band filtering functions; those single-band filtering functions can be obtained using the technique in [1]. Based on our proposed method, the fully analytical fractional expressions for two-port scattering parameters are generated. Moreover, under proper combination, the prescribed transmission zeros are available in multiband filters, while the different bandwidth of each passband is also allowed. Once the fractional forms for the scattering parameters of the dual-band or multiband filtering function are obtained, they are converted into the transversal coupling matrix using the method in [3]. Using the technique in [5], the transversal coupling matrix can be transferred into a requested coupling scheme.

To verify the proposed method, the parallel-coupled filter structure, described in [16], is chosen to realize the dual-band filters based on the dual-band coupling matrix. For the dual-band filter implementation, the technique in [17] has been proposed. However, it is not easy to be implemented in the microstrip technology. For the microstrip implementation, single-path and dual-path dual-band coupling schemes are discussed. Finally, we will provide two microstrip parallel-coupled dual-band filters as examples and show the feasibility of the proposed synthesis technique. Moreover, we will also demonstrate that both single-path and dual-path dual-band coupling schemes are useful in dual-band filter designs.

II. Analytical Transversal Coupling Matrix Synthesis for Multiband Filter Design

For a two-port lossless filter network with N intercoupled resonators, the transfer and reflection function can be expressed as a ratio of two Nth degree polynomials

$$S_{11}(\omega) = \frac{F_N(\omega)}{E_N(\omega)} \quad S_{21}(\omega) = \frac{P_N(\omega)}{\varepsilon E_N(\omega)} \tag{1}$$

where ω is the real frequency variable, the related complex frequency variable $s = j\omega$, and ε is a normalization constant re-

Manuscript received December 01, 2009; revised March 04, 2010; accepted April 03, 2010. Date of publication June 07, 2010; date of current version July 14, 2010.

Y.-T. Kuo and C.-Y. Chang are with the Department of Electrical Engineering, National Chiao Tung University, Hsinchu 300, Taiwan (e-mail: erickuo.cm93g@nctu.edu.tw; mhchang@cc.nctu.edu.tw).

J.-C. Lu is with the Taiwan Semiconductor Manufacturing Company, Ltd., Hsinchu 303, Taiwan (e-mail: zill_gerching@hotmail.com).

C.-K. Liao is with the Gemtek Technology Company Ltd., Hsinchu 303, Taiwan (e-mail: Ching_Liao@gemtek.com.tw).

Color versions of one or more of the figures in this paper are available online at http://ieeexplore.iee.org.

Digital Object Identifier 10.1109/TMTT.2010.2050240

lated to the prescribed return loss level; all polynomials have been normalized so that their highest degree coefficients are unity. $S_{11}(\omega)$ and $S_{21}(\omega)$ have a common denominator $E_N(\omega)$; the transmission zeros of the transfer function are contained in the polynomial $P_N(\omega)$. Using (1) and the energy conservation for a lossless network, $S_{11}(\omega)^2 + S_{21}(\omega)^2 = 1$, $S_{21}(\omega)$ can be represented as

$$S_{21}(\omega)^2 = \frac{1}{1+\varepsilon^2 C_N^2(\omega)} \tag{2}$$

where

$$C_N(\omega) = \frac{F_N(\omega)}{P_N(\omega)}. \tag{3}$$

$C_N(\omega)$ is known as the filtering function of degree N. Here, the proposed filters have the form of the generalized Chebyshev characteristic. A filtering function for a single-band filter can be synthesized with an efficient recursive procedure. Based on this, the aim is now to design a filtering function for multiband filters. The proposed multiband polynomial synthesis discussed below will be fully analytical using single-band filtering functions.

Using the property of the generalized Chebyshev characteristic in (3), the reciprocal of the filtering function for a dual-band filter can be achieved by summing up the reciprocal of two frequency-shifted single-band filtering functions. The value of C_N in the passband is much smaller than that in the out-of-band, the reciprocal value of C_N in the passband can then be kept after summing up the reciprocal of the value of other C_N in the out-of-band. Finally, the composite filtering function can be obtained as follows:

$$C_N(\omega) = \frac{1}{\frac{1}{C_{N1}(\omega)} + \frac{1}{C_{N2}(\omega)}} = \frac{C_{N1}(\omega)C_{N2}(\omega)}{C_{N1}(\omega) + C_{N2}(\omega)}. \tag{4}$$

The principal advantage of this technique is that the individual filtering functions C_{N1} and C_{N2} can be obtained analytically by the efficient recursive technique. The polynomial of the composite filtering function can then be derived as

$$\begin{aligned} C_N(\omega) &= \frac{1}{\frac{1}{C_{N1}(\omega)} + \frac{1}{C_{N2}(\omega)}} \\ &= \frac{1}{\frac{P_{N1}(\omega)}{F_{N1}(\omega)} + \frac{P_{N2}(\omega)}{F_{N2}(\omega)}} \\ &= \frac{F_{N1}(\omega)F_{N2}(\omega)}{P_{N1}(\omega)F_{N2}(\omega) + P_{N2}(\omega)F_{N1}(\omega)} \\ &= \frac{F_N(\omega)}{P_N(\omega)} \end{aligned} \tag{5}$$

where $F_{N1}(\omega)$, $F_{N2}(\omega)$, $P_{N1}(\omega)$, and $P_{N2}(\omega)$ are generated by frequency shifting of the original filtering function through

$$\begin{aligned} F_{Ni}(\omega) &= F'_{Ni}(\omega - \omega_{si}) \\ P_{Ni}(\omega) &= P'_{Ni}(\omega - \omega_{si}) \end{aligned} \tag{6}$$

where $i = 1$ and 2, ω_{si} is the central frequency for the ith passband, and $F'_{Ni}(\omega)$ and $P'_{Ni}(\omega)$ are all generated by the recursive technology analytically [1]–[4]. In addition, the transmission zeros can be generated using those C_{N1} and C_{N2} corresponding to their central frequency at each passband via (5).

To use the different bandwidths of each passband, these polynomials should be modified. For the ith filtering function with frequency shift ω_{si}, the polynomials can be represented as

$$\begin{aligned} P_{Ni}(\omega) &= \prod_{j=1}^{NP_i} (\mathrm{BW}_i \cdot (\omega - \omega_{si}) - p_{i,j}) \\ F_{Ni}(\omega) &= \prod_{j=1}^{NF_i} (\mathrm{BW}_i \cdot (\omega - \omega_{si}) - f_{i,j}) \end{aligned} \tag{7}$$

where P_{Ni} is the denominator and F_{Ni} is the numerator of C_{Ni}, $p_{i,j}$ is the jth root of P_{Ni} and $f_{i,j}$ is the jth root of F_{Ni}, and NP_i and NF_i are the number of roots of P_{Ni} and F_{Ni}. Based on (7), the bandwidth of the scaled polynomial will be $1/\mathrm{BW}$ times the bandwidth of the original one.

For the multiband filter design, suppose there are m passbands for a filter and that all of the filtering functions are C_{N1}, $C_{N2}, \ldots,$ and C_{Nm}, so that the composite filtering function can then be calculated as follows:

$$\begin{aligned} C_N(\omega) &= \frac{1}{\frac{1}{C_{N1}(\omega)} + \frac{1}{C_{N2}(\omega)} + \cdots + \frac{1}{C_{Nm}(\omega)}} \\ &= \frac{F_{N1}(\omega)F_{N2}(\omega)\cdots F_{Nm}(\omega)}{\sum_{i=1}^{m}\left(P_{Ni}(\omega)\prod_{\substack{j=1\\ j\neq i}}^{m} F_{Nj}(\omega)\right)} \end{aligned} \tag{8}$$

where P_{Ni} is the numerator and F_{Ni} is the denominator of C_{Ni}. Here, each passband has the individual filter order and the number of transmission zeros. By carefully placing the transmission zeros, the requested frequency response can be obtained under desired specifications.

The bandwidth of each passband, however, is 2 rad/s, corresponding to the Chebyshev characteristic, so that the edges of passbands are out of ± 1 rad/s. To normalize the edges of passbands within ± 1 rad/s, let ω be the original frequency, ω' be the normalized frequency, ω_H be the upper edge of passbands, and ω_L be the lower edge of passbands. The frequency transformation is

$$\omega' = \frac{2}{\omega_H - \omega_L}(\omega - \omega_H) + 1 \tag{9}$$

where ω_H and ω_L are the edges of passbands in the original frequency domain. After the frequency transformation, the polynomials derived in (8) are then transferred into the normalized frequency domain. Finally, the transversal coupling matrix based on the generated polynomials is obtained using the method in [3].

To transfer the response to the bandpass domain, the following equation is used:

$$\begin{aligned} \omega_{LP} &= \frac{\omega_{C,\mathrm{BP}}}{\omega_{H,\mathrm{BP}} - \omega_{L,\mathrm{BP}}}\left(\frac{\omega_{\mathrm{BP}}}{\omega_{C,\mathrm{BP}}} - \frac{\omega_{C,\mathrm{BP}}}{\omega_{\mathrm{BP}}}\right) \\ &= \frac{1}{\Delta}\left(\frac{\omega_{\mathrm{BP}}}{\omega_{C,\mathrm{BP}}} - \frac{\omega_{C,\mathrm{BP}}}{\omega_{\mathrm{BP}}}\right) \end{aligned} \tag{10}$$

where ω_{LP} is the frequency in the low-pass domain, ω_{BP} is the frequency in the bandpass domain, $\omega_{C,\mathrm{BP}}$, $\omega_{H,\mathrm{BP}}$, and $\omega_{L,\mathrm{BP}}$ are the central frequency, the upper edge of passbands, and the

lower edge of passbands in the bandpass domain, respectively, and Δ is the fractional bandwidth.

In the following sections, three examples are given to demonstrate the proposed method.

A. Symmetrical Dual-Band Bandpass Filters

In this example, the specifications of a symmetrical dual-band bandpass filter are provided. Two passbands both have filter order 3. The first passband has a central frequency at 2.32 GHz and the fractional bandwidth is 5%. The second passband has a central frequency at 2.695 GHz and the fractional bandwidth is 5%. The transmission zeros are 2.122, 2.5, and 2.945 GHz. Hence, the lower edge of the first passband is $2.32 \times (1 - 0.05) = 2.262$ GHz and the upper edge of the second passband is $2.695 \times (1 + 0.05) = 2.7624$ GHz, so that the central frequency is about $(2.262 + 2.7624)/2 \approx 2.5$ GHz, and the fractional bandwidth is about $(2.7624 - 2.262)/2.5 \approx 20\%$. To transfer the response form the bandpass domain to the low-pass domain using (10), the normalized central frequencies are about $-0.75$and 0.75 rad/s, and the normalized transmission zeros are about -1.65 and 1.65 rad/s.

Based on the above frequencies in the normalized domain, the requested two filtering functions are expressed as follows. One is the third-order filtering function, which has the normalized central frequency at -0.75 rad/s and the normalized transmission zeros at -1.5 rad/s. The other one is the third-order filtering function, which has the normalized central frequency at 0.75 rad/s and the normalized transmission zeros at 1.5 rad/s. Hence, the transmission zeros of the composite filtering function are almost -1.65, 0, and 1.65 rad/s, which meet the requested specifications. The in-band return loss level is 20 dB for these two filtering functions.

To combine these two filtering functions, the frequency transformation in (9) is needed first. The bandwidth of the passband in original domain in (9) is 2 rad/s (i.e., -1 to 1 rad/s), so that the bandwidth between the central frequency and the edge of passband within each passband is 1 rad/s. The requested bandwidth between the normalized central frequency and the edge of passband within each passband is $(1 - 0.75 = 0.25)$ rad/s. To transfer the normalized response to the original frequency using (9), the factor which times the normalized frequency is 4, so that the central frequencies after the frequency transformation are $(-0.75 \times 4) = -3$ and $(0.75 \times 4) = 3$ rad/s, and transmission zeros are $(\pm 1.5 \times 4) = \pm 6$ rad/s. Finally, combining these two filtering functions using (5) and transfer the response into the normalized frequency domain using (9).

The transmission zeros of the composite filtering function are slightly shifted, and this can be noted in Fig. 1(a). The frequency shift comes from the combination of two filtering functions and can be eliminated by careful designing these two filtering functions. Fig. 1(b) shows the corresponding S-parameters. In this figure, an additional transmission zero is 0 rad/s. This is because the phase of C_{N1} and C_{N2} is 180 degree out-of-phase around 0 rad/s, and then an additional zero is introduced, as shown in Fig. 1. Furthermore, the transversal coupling matrix is obtained based on the derived polynomials and is shown in Table I.

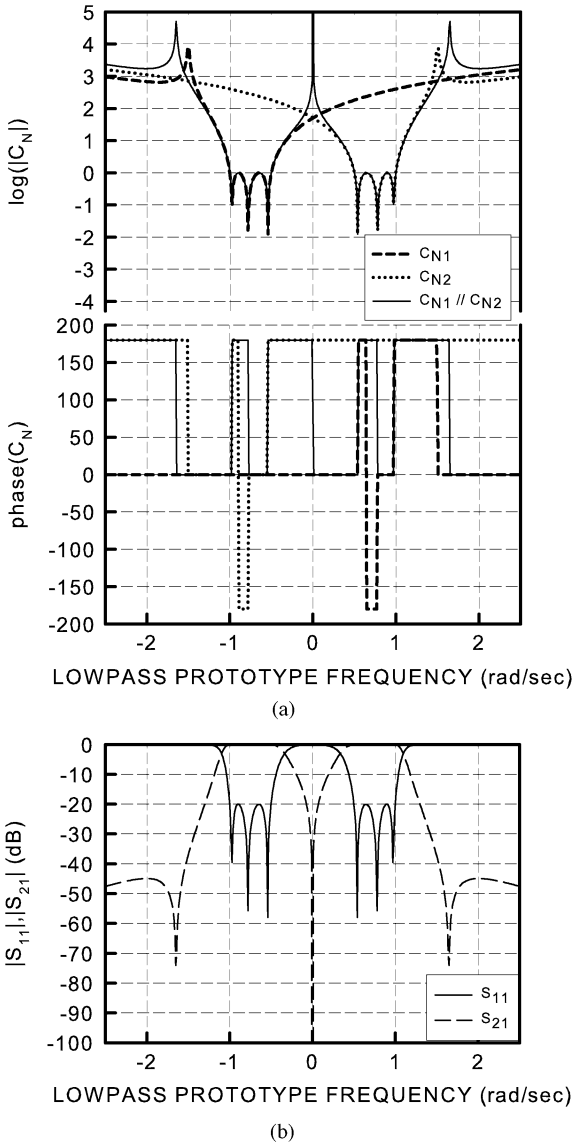

Fig. 1. (a) Filtering functions for two single-band filters of same degrees 3 (C_{N1} has the transmission zero at -1.5 and the central frequency -0.75 rad/s) and (C_{N2} has the transmission zero at 1.5 rad/s and the central frequency 0.75 rad/s), and the composite dual-band filter $(C_{N1}//C_{N2})$. The in-band return loss level is 20 dB in each case. (b) Corresponding S_{11} and S_{21} for the symmetric dual-band filter.

TABLE I
COUPLING MATRIX FOR THE FILTER IN FIG. 1

	S	1	2	3	4	5	6	L
S	0.0	0.2432	-0.3811	0.2933	0.2933	-0.3811	0.2432	0.0
1	0.2432	1.1169	0.0	0.0	0.0	0.0	0.0	0.2432
2	-0.3811	0.0	0.8712	0.0	0.0	0.0	0.0	0.3811
3	0.2933	0.0	0.0	0.4212	0.0	0.0	0.0	0.2933
4	0.2933	0.0	0.0	0.0	-0.4212	0.0	0.0	0.2933
5	-0.3811	0.0	0.0	0.0	0.0	-0.8712	0.0	0.3811
6	0.2432	0.0	0.0	0.0	0.0	0.0	-1.1169	0.2432
L	0.0	0.2432	0.3811	0.2933	0.2933	0.3811	0.2432	0.0

B. Asymmetrical Dual-Band Bandpass Filters

For an asymmetrical dual-band bandpass filter, the frequency response is not symmetric about the central frequency. Two filtering functions used to illustrate the dual-band characteristic have following specifications. One is the third-order func-

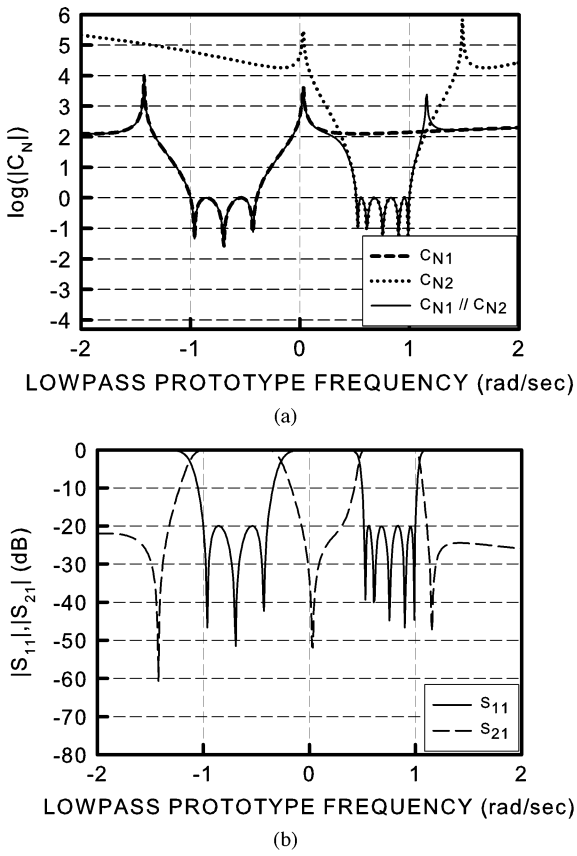

Fig. 2. (a) Filtering functions for two single-band filters of different degrees 3 (C_{N1} has transmission zeros at -1.4242 and 0 rad/s and the central frequency -0.6970 rad/s. Its bandwidth factor is 0.8) and 5 (C_{N2} has transmission zeros at 0 and 1.4848 rad/s and the central frequency 0.7576 rad/s), and the composite dual-band filter ($C_{N1}//C_{N2}$). The in-band return loss level is 20 dB in each case. (b) Corresponding S_{11} and S_{21} for the asymmetric dual-band filter.

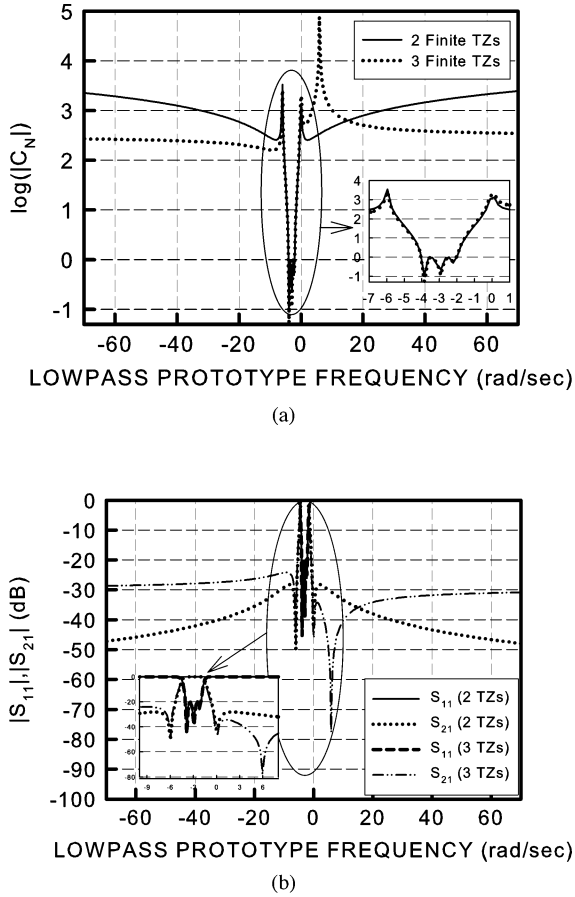

Fig. 3. (a) Two third-order filtering functions. Solid line: filtering function has two finite transmission zeros at -6 and 0 rad/s, and the central frequency is -3 rad/s. Dashed line: filtering function with 3 finite transmission zeros at -6, 0 and 6 rad/s, and the central frequency is -3 rad/s. The in-band return loss level is 20 dB in each case. (b) The corresponding S_{11} and S_{21}.

TABLE II
COUPLING MATRIX FOR THE FILTER IN FIG. 2

	S	1	2	3	4	5	6	7	8	L
S	0.0	-0.2666	0.4510	-0.2535	-0.1534	0.2318	-0.2586	0.2720	-0.1834	0.0
1	-0.2666	1.1433	0.0	0.0	0.0	0.0	0.0	0.0	0.0	0.2666
2	0.4510	0.0	0.7658	0.0	0.0	0.0	0.0	0.0	0.0	0.4510
3	-0.2535	0.0	0.0	0.3006	0.0	0.0	0.0	0.0	0.0	0.2535
4	-0.1534	0.0	0.0	0.0	-0.4716	0.0	0.0	0.0	0.0	0.1534
5	0.2318	0.0	0.0	0.0	0.0	-0.5766	0.0	0.0	0.0	0.2318
6	-0.2586	0.0	0.0	0.0	0.0	0.0	-0.7900	0.0	0.0	0.2586
7	0.2720	0.0	0.0	0.0	0.0	0.0	0.0	-1.0005	0.0	0.2720
8	-0.1834	0.0	0.0	0.0	0.0	0.0	0.0	0.0	-1.0680	0.1834
L	0.0	0.2666	0.4510	0.2535	0.1534	0.2318	0.2586	0.2720	0.1834	0.0

tion, which has the normalized central frequency at -0.6970 rad/s and normalized transmission zeros at -1.4242 and 0 rad/s, and its bandwidth factor BW in (7) is 0.8. The other one is the fifth-order function, and it has the normalized frequency at 0.7576 rad/s and the normalized transmission zeros at 0 and 1.4848 rad/s. The corresponding responses for these two filtering functions are shown in Fig. 2. After combining these two filtering functions, the response for the asymmetric dual-band filter is shown in Fig. 2 with the coupling matrix in Table II.

It is noted, however, that the transmission zero on the upper stopband of the composite filtering function is seriously influenced by the filtering function C_{N1}. Because the filtering function C_{N1} has a lower order, the function value at the out-of-band is smaller than that of C_{N2}. To compute the composite filtering function using (4), the filtering function with smaller value will dominate the response of the composite filtering function. Hence, the transmission zero on the upper stopband of the composite filtering function shifts inward with respect to the transmission zero of C_{N2}. This can be overcome by preadjusting the zero of C_{N2} to a higher frequency or by the method described in the following paragraph.

The alternative method to overcome the zero shifting problems is to take advantage of the generalized Chebyshev characteristic, that is, for an Nth-order filtering function, the number of transmission zeros can be smaller than or equal to N. When the number of transmission zeros is equal to N, it implies no infinite transmission zeros. Fig. 3 shows an example, where TZs in the figure denotes the abbreviation of transmission zeros.

In this case, these two filtering functions with same order 3 have transmission zeros at (-6 and 0) rad/s and (-6, 0, and 6) rad/s respectively, and have the central frequency at -3 rad/s, respectively. The filtering function with three transmission zeros has no infinite transmission zero, so the stopband rejection is worse due to no infinite transmission zeros. The stopband rejection, however, can still be kept under an acceptable level. As shown in Fig. 3, the filtering function with three transmission zeros has the logarithm value close to 2.5 even the frequency up to 60 rad/s, which is -30 dB in S_{21}.

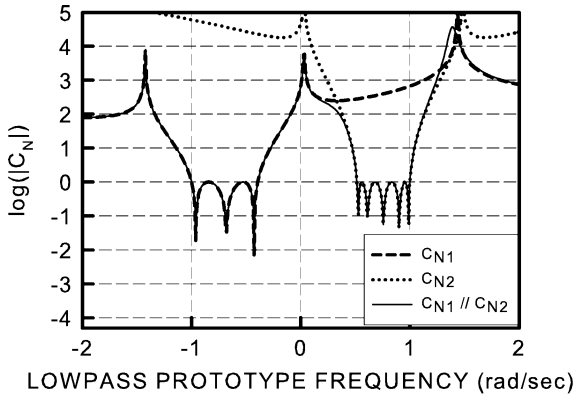

(a)

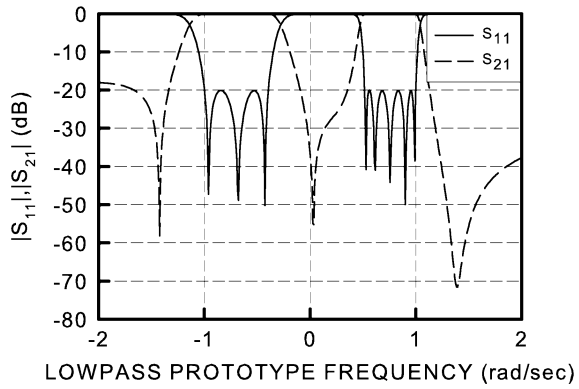

(b)

Fig. 4. (a) Filtering functions for two single-band filters of different degrees 3 (C_{N1} has transmission zeros at -1.4242, 0, and 1.4848 rad/s and the central frequency -0.6970 rad/s. Its bandwidth factor is 0.8), and 5 (C_{N2} has transmission zeros at 0 and 1.5091 rad/s and the central frequency 0.7576 rad/s), and the composite dual-band filter ($C_{N1}//C_{N2}$). The in-band return loss level is 20 dB in each case. (b) The corresponding S_{11} and S_{21} for the asymmetric dual-band filter with adjustable upper transmission zero.

Use the above property, the example for asymmetric dual-band filter is modified. Fig. 4 shows the modification. One third-order filtering function C_{N1} has normalized transmission zeros at -1.4242, 0, and 1.4848 rad/s, and it has the normalized central frequency at -0.6970 rad/s. Its bandwidth factor is 0.8. The other one is the fifth-order filtering function C_{N2}, which has normalized transmission zeros at 0 and 1.5091 rad/s, and the normalized central frequency is 0.7576 rad/s. In this case, the transmission zero at 1.4848 rad/s of C_{N1} precisely locates the transmission zero on the upper stopband for the composite filtering function. Table III shows the corresponding coupling matrix. Compared with the result in Fig. 2, the upper stopband transmission zero can be precisely located.

C. Multiband Bandpass Filters

In this example a four-band filter is provided. There are four filtering functions in this example: 1) third-order fithering function C_{N1} with normalized transmission zeros at -1.2 and -0.6 rad/s and the normalized central frequency at -0.9 rad/s;

TABLE III
COUPLING MATRIX FOR THE FILTER IN FIG. 4

	S	1	2	3	4	5	6	7	8	L
S	0.0	-0.2764	0.4533	-0.2407	-0.1515	0.2335	-0.2597	0.2685	-0.1916	0.0338
1	-0.2764	1.1500	0.0	0.0	0.0	0.0	0.0	0.0	0.0	0.2750
2	0.4533	0.0	0.7293	0.0	0.0	0.0	0.0	0.0	0.0	0.4522
3	-0.2407	0.0	0.0	0.3039	0.0	0.0	0.0	0.0	0.0	0.2399
4	-0.1515	0.0	0.0	0.0	-0.4720	0.0	0.0	0.0	0.0	0.1508
5	0.2335	0.0	0.0	0.0	0.0	-0.5763	0.0	0.0	0.0	0.2330
6	-0.2597	0.0	0.0	0.0	0.0	0.0	-0.7895	0.0	0.0	0.2591
7	0.2685	0.0	0.0	0.0	0.0	0.0	0.0	-0.9989	0.0	0.2679
8	-0.1916	0.0	0.0	0.0	0.0	0.0	0.0	0.0	-1.0699	0.1886
L	0.0338	0.2750	0.4522	0.2399	0.1508	0.2330	0.2591	0.2679	0.1886	0.0

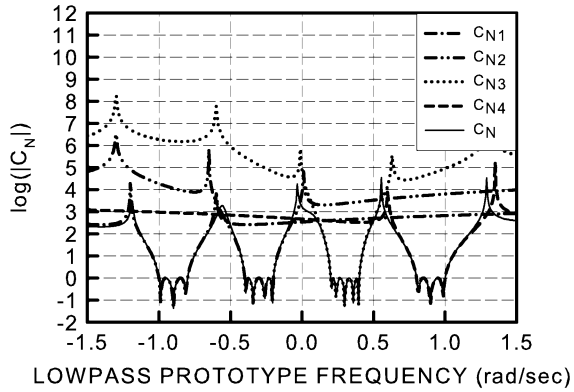

(a)

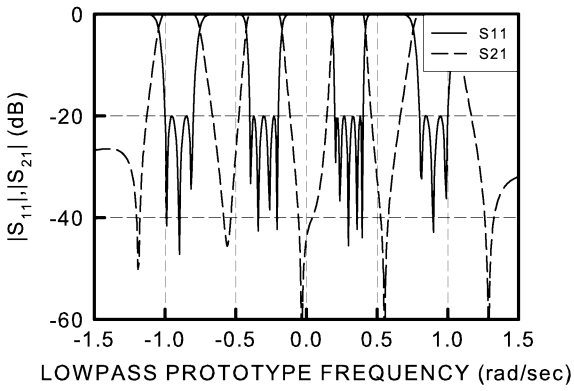

(b)

Fig. 5. (a) Filtering functions for four single-band filters of degree 3 (C_{N1} has transmission zeros at -1.2 and 0.6 rad/s and the central frequency at -0.9 rad/s), degree 4 (C_{N2} has transmission zeros at -1.3, -0.65, and 0.01 rad/s and the central frequency at -0.3 rad/s), degree 5 (C_{N3} has transmission zeros at -1.3, -0.6, -0.01, 0.63, and 1.3 rad/s and the central frequency at 0.3 rad/s), and degree 3 (C_{N4} has transmission zeros at 0.45 and 0.9 rad/s and the central frequency at 0.9 rad/s), and the composite quad-band filter ($C_{N1}//C_{N2}//C_{N3}//C_{N4}$). The in-band return loss level is 20 dB in each case. (b) The corresponding S_{11} and S_{21} for the quad-band filter.

2) fourth-order C_{N2} with normalized transmission zeros at -1.3, -0.65 and 0.01 rad/s and the normalized central frequency at -0.3 rad/s; 3) fifth-order C_{N3} with normalized transmission zeros at -1.3, -0.6, -0.01, 0.63, and 1.3 rad/s and the normalized central frequency at 0.3 rad/s; and 4) third-order C_{N4} with normalized transmission zeros at 0.45 and 0.9 rad/s and the normalized frequency at 0.9 rad/s. Fig. 5 shows the frequency response. In this case, the lower order filtering functions (i.e., C_{N1} and C_{N4}) are used to adjust the transmission zeros to specific locations, while the other filtering functions are used to be slightly tuned for the specific locations

TABLE IV
COUPLING MATRIX FOR THE FILTER IN FIG. 5

$M_{S,1}$	-0.1695	$M_{S,2}$	0.2604	$M_{S,3}$	-0.1560	$M_{S,4}$	0.1212
$M_{S,5}$	-0.1876	$M_{S,6}$	0.1874	$M_{S,7}$	-0.1195	$M_{S,8}$	-0.0983
$M_{S,9}$	0.1501	$M_{S,10}$	-0.1632	$M_{S,11}$	0.1591	$M_{S,12}$	-0.1085
$M_{S,13}$	-0.1508	$M_{S,14}$	0.2565	$M_{S,15}$	-0.1818	$M_{1,L}$	0.1695
$M_{2,L}$	0.2604	$M_{3,L}$	0.1560	$M_{4,L}$	0.1212	$M_{5,L}$	0.1876
$M_{6,L}$	0.1874	$M_{7,L}$	0.1195	$M_{8,L}$	0.0983	$M_{9,L}$	0.1501
$M_{10,L}$	0.1632	$M_{11,L}$	0.1591	$M_{12,L}$	0.1085	$M_{13,L}$	0.1508
$M_{14,L}$	0.2565	$M_{15,L}$	0.1818	$M_{1,1}$	1.0576	$M_{2,2}$	0.9416
$M_{3,3}$	0.7761	$M_{4,4}$	0.4298	$M_{5,5}$	0.3688	$M_{6,6}$	0.2458
$M_{7,7}$	0.1736	$M_{8,8}$	-0.1802	$M_{9,9}$	-0.2174	$M_{10,10}$	-0.3014
$M_{11,11}$	-0.3875	$M_{12,12}$	-0.4242	$M_{13,13}$	-0.7758	$M_{14,14}$	-0.9307
$M_{15,15}$	-1.0624						

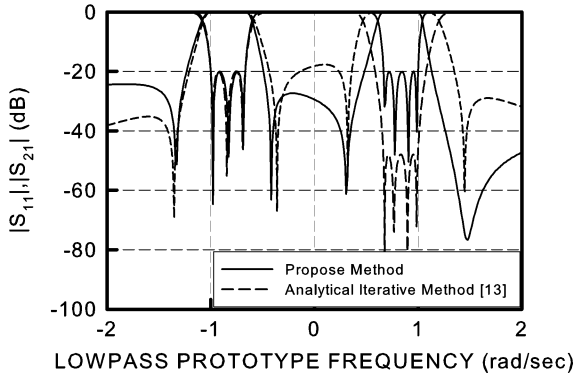

Fig. 6. Frequency responses of the dual-band filter composed of the third- and fourth-order filtering functions. Solid line: the proposed method. Dashed line: the analytical iterative method.

of transmission zeros. Table IV shows the corresponding coupling matrix. The matrix elements not listed in Table IV are all zero.

III. COMPARISON WITH OTHER METHOD

In the coupling matrix synthesis of the dual-band or multiband filter, the most popular and efficient analytical method is the analytical iterative method [13]. This method has features of user-defined number of passbands, number of transmission zeros, return loss level, range of each passband and stopband, and prescribed imaginary or complex transmission zeros. By efficient iterative procedure, the transmission zeros are extracted, and some fine tunes are needed if prescribed real transmission zeros are requested. The equal-ripple levels in different passbands are not necessarily identical but can be achieved by run-and-try process. The difference of return loss levels in different passbands, however, becomes large with consideration of different filter orders in different passbands.

Compare the proposed method to the analytical iterative method, the above features of the iterative method are also the features of the proposed method. Moreover, the equal-ripple levels in different passbands are preserved. Here an example is given to show the differences between these two methods. The specifications are listed in Table V, and the requested return loss is 20 dB in both passbands for this example. The frequency responses obtained by these two methods are shown in Fig. 6.

In Fig. 6, the responses of the passband with third-order are similar from two methods. For the passband with fourth order,

TABLE V
SPECIFICATIONS USED IN FIG. 6

Passband	# of poles	Stopband	# of zeros	Prescribed zeros
-1.0 to -0.6661	3	$-\infty$ to -1.3	1	none
0.6661 to 1.0	4	-0.45 to 0.37	2	
		1.4 to ∞	1	

due to the equal-ripple preservation in the proposed method, the return loss level is kept to be 20 dB, while the return loss level is 50 dB from the iterative method. Hence, the second passband from the iterative method has wider bandwidth than that from the proposed method if the return loss level 20 dB is used. Hence, for the filter composed of filtering functions with different orders, the proposed method hold the equal-ripple property.

To check the transmission zeros from two methods, due to the parallel addition in the proposed method, the number of transmission zeros will increase. The transmission zeros are -1, 3528, -0.3589, 0.3232, and 1.4496 rad/s in the iterative method, while they are -1, 333, -0.4151, 0.3099, $0.7936 \pm 0.5468j$, and $1.4694 \pm 0.047j$ rad/s in the proposed method. Although the additional complex prescribed transmission zeros $0.7936 \pm 0.5468j$ can be added in the iterative method to pull back the return loss level from 50 to 30 dB, but it is difficult to know the prescribed zeros in order to pull back the return loss.

For the filter composed of filtering functions with same filter order, the iterative method has the advantage in the specification assignment. The only thing the designer needs to do is to assign the range of each passband and each stopband, number of poles and zeros, and the return loss level, so that the corresponding polynomials are generated. For the proposed method, the designer needs to assign the locations of transmission zeros first in order to design the characteristic of multiband filter. These two methods, however, both can analytically generate the coupling matrix for the multiband filter. For the filter composed of filtering functions with different filter orders, the proposed method provides an alternative way to synthesis the multiband filter with the equal-ripple property.

IV. CROSS-COUPLING SCHEMES AND FILTER DESIGN EXAMPLES

The planar microstrip filter with finite transmission zeros has been proposed systematically in [16]. The method in [16] is modified here for the dual-band filter. In this section, two types of coupling schemes are proposed to realize dual-band filters and simplify the complexity of the hardware implementation in the microstrip technology. First is a single-path coupling scheme and second is a dual-path coupling scheme.

A. Example 1: Single-Path Dual-Band Coupling Scheme

In the single-band filter design, the cross-coupling path helps in the generation of the finite transmission zeros. The trisection and quadruplet coupling schemes are known to exhibit the highly selective responses. To apply trisection and quadruplet to the dual-band design in the single-path coupling scheme, finite transmission zeros will be placed to separate two passbands. For example, a dual-band filter is designed to have two second-order

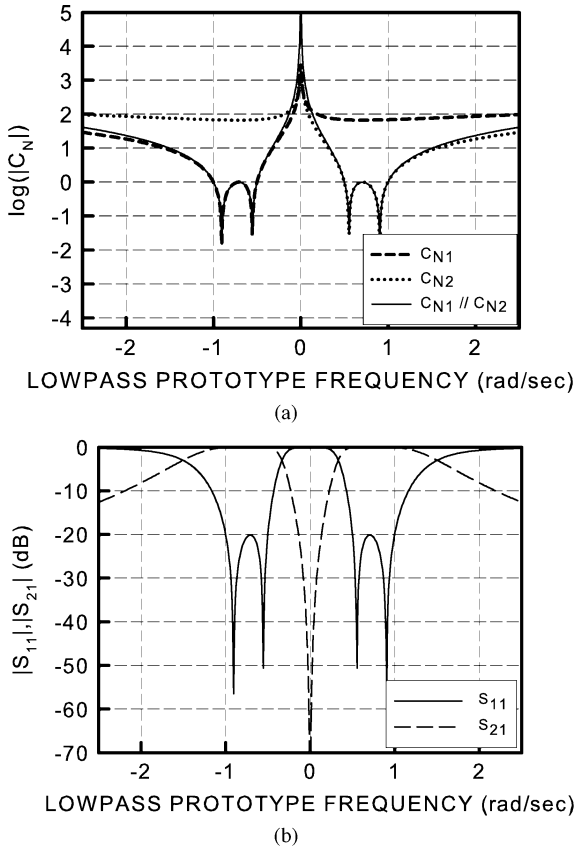

Fig. 7. (a) Filtering functions for two single-band filters of degree 2 (C_{N1} has the transmission zero at 0 rad/s and the central frequency at -0.75 rad/s, and C_{N2} has the transmission zero at 0 rad/s and the central frequency at 0.75 rad/s), and the composite dual-band filter ($C_{N1}//C_{N2}$) The in-band return loss level is 20 dB in each case. (b) The corresponding S_{11} and S_{21} for the dual-band filter in example 1.

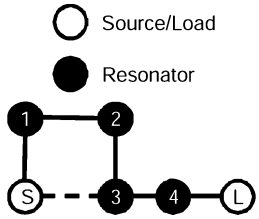

Fig. 8. Single-path coupling scheme in example 1.

filtering functions; one has a normalized transmission zero at 0 rad/s and the normalized central frequency at 0.75 rad/s, while the other one has a normalized transmission zero at 0 rad/s and the normalized central frequency at -0.75 rad/s. The synthesized filtering functions and corresponding S-parameters are shown in Fig. 7.

The transversal coupling matrix is shown in Table VI. Due to two transmission zeros from each passband are used to contribute the separation of two passbands, the quadruplet topology is used. In order to convert the transversal coupling matrix for the single-path coupling scheme with quadruplet coupling scheme, the optimization procedure proposed in [5] is used. The coupling scheme is shown in Fig. 8 and the corresponding coupling matrix is listed in Table VII.

TABLE VI
TRANSVERSAL COUPLING MATRIX FOR THE DUAL-BAND FILTER IN EXAMPLE 1

	S	1	2	3	4	L
S	0.0	0.5315	-0.3046	0.3046	-0.5315	0.0
1	0.5315	1.2338	0.0	0.0	0.0	0.5315
2	-0.3046	0.0	0.4053	0.0	0.0	0.3046
3	0.3046	0.0	0.0	-0.4053	0.0	0.3046
4	-0.5315	0.0	0.0	0.0	-1.2338	0.5315
L	0.0	0.5315	0.3046	0.3046	0.5315	0.0

TABLE VII
COUPLING MATRIX FOR DUAL-BAND FILTER IN EXAMPLE 1 WITH THE COUPLING SCHEME SHOWN IN FIG. 8

	S	1	2	3	4	L
S	0.0	0.5624	0.0	0.6590	0.0	0.0
1	0.5624	0.0	0.4590	0.0	0.0	0.0
2	0.0	0.4590	0.0	0.5379	0.0	0.0
3	0.6590	0.0	0.5379	0.0	1.0893	0.0
4	0.0	0.0	0.0	1.0893	0.0	0.8663
L	0.0	0.0	0.0	0.0	0.8663	0.0

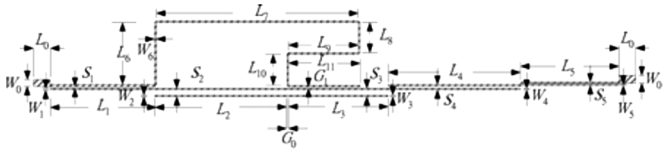

Fig. 9. Layout in example 1.

TABLE VIII
DIMENSIONS IN EXAMPLE 1 (IN MILLIMETERS)

W_0	W_1	W_2	W_3	W_4	W_5	W_6	L_0
1.1180	0.2540	0.2540	0.2540	0.3302	0.2032	0.2032	2.5400
L_1	L_2	L_3	L_4	L_5	L_6	L_7	L_8
16.7400	20.8500	15.7700	21.0600	15.7200	10.1600	32.1300	4.9780
L_9	L_{10}	L_{11}	S_1	S_2	S_3	S_4	S_5
11.2300	5.0800	11.4300	0.2540	0.8382	0.8382	0.2540	0.2032
G_0	G_1						
0.2540	0.2032						

The central frequencies of the two passbands in the practical design are 2.3 and 2.7 GHz, while the fractional bandwidth is 5% in each passband. For the practical implementation, a 0.508-mm-thick Rogers RO4003 substrate with a relative dielectric constant 3.58 and a loss tangent of 0.0021 is used. Based on the design procedure in [16], the layout of the proposed microstrip filter is shown in Fig. 9. The dimensions are listed in Table VIII.

B. Example 2: Dual-Path Dual-Band Coupling Scheme

For the dual-band filter design, the single-path coupling scheme do not have an obvious relationship with the dual-band characteristics. To relate each passband with coupling topology, the dual-path coupling scheme is considered. For example, there are two filtering functions; One is the 3rd order filtering function, which has normalized transmission zero at -1.8 rad/s and normalized central frequency at -0.8 rad/s, while the other is the 3rd order filtering function, which has normalized transmission zero at 1.8 rad/s and normalized central frequency at 0.8 rad/s. The synthesized filtering functions and the corresponding S-parameters are shown in Fig. 10. The transversal coupling matrix in this example is listed in Table IX.

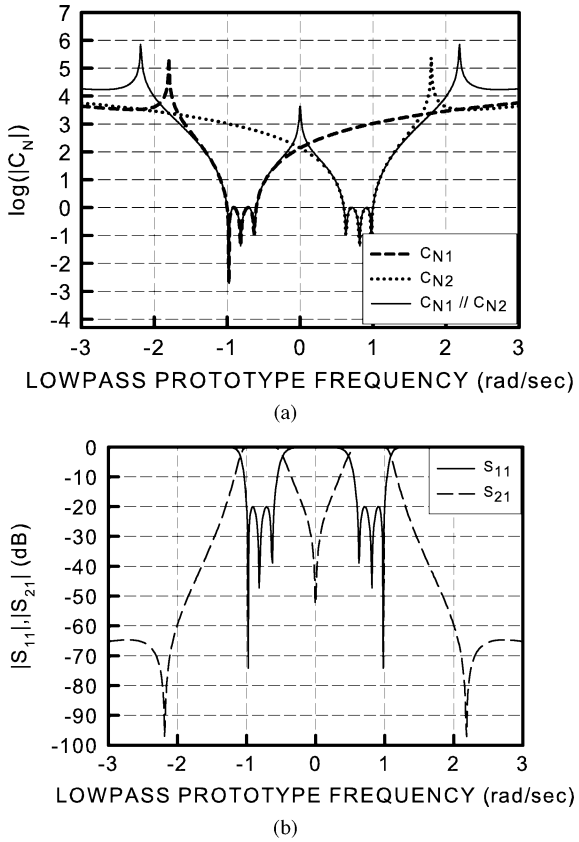

Fig. 10. (a) Filtering functions for two single-band filters of degree 3 (C_{N1} has the transmission zero at -1.8 rad/s and the central frequency at -0.8 rad/s, and C_{N2} has the transmission zero at 1.8 rad/s and the central frequency at 0.8 rad/s), and the composite filter ($C_{N1}//C_{N2}$). The in-band return loss level is 20 dB in each case. (b) The corresponding S_{11} and S_{21} for the dual-band filter in example 2.

TABLE IX
TRANSVERSAL COUPLING MATRIX FOR THE DUAL-BAND FILTER IN EXAMPLE 2

	S	1	2	3	4	5	6	L
S	0.0	0.2295	-0.3419	0.2534	0.2534	-0.3419	0.2295	0.0
1	0.2295	1.0975	0.0	0.0	0.0	0.0	0.0	0.2295
2	-0.3419	0.0	0.8653	0.0	0.0	0.0	0.0	0.3419
3	0.2534	0.0	0.0	0.5272	0.0	0.0	0.0	0.2534
4	0.2534	0.0	0.0	0.0	-0.5272	0.0	0.0	0.2534
5	-0.3419	0.0	0.0	0.0	0.0	-0.8653	0.0	0.3419
6	0.2295	0.0	0.0	0.0	0.0	0.0	-1.0975	0.2295
L	0.0	0.2295	0.3419	0.2534	0.2534	0.3419	0.2295	0.0

The transmission zero for the separation of two passbands is created as demonstrated in the discussion in Section II-A. In this case, there are three finite transmission zeros within the entire low-pass domain; these are -1.8, 0 and 1.8 rad/s. To illustrate the dual-band characteristic and let each path govern one passband, the trisection portion of each path is used to provide one transmission zero on the stopband. Fig. 11 shows the coupling scheme, and the corresponding coupling matrix is rotated by following steps [4]. The values of diagonal elements of the transversal matrix are categorized into two groups, which are positive values and negative values, and then the original matrix can be separated into two parts with values shown in Table X. Based on these two sub-matrices, the rotation sequence in Table XI are applied and then the matrix for the coupling scheme in Fig. 11 are extracted with values listed in Table XII.

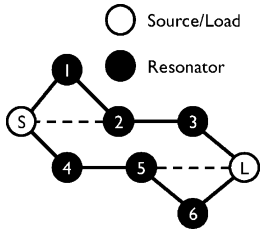

Fig. 11. Dual-path coupling scheme in example 2.

TABLE X
(A) TRANSVERSAL COUPLING MATRIX FOR THE UPPER PATH (M1). (B) TRANSVERSAL COUPLING MATRIX FOR THE LOWER PATH (M2)

(a)

	S	1	2	3	L
S	0.0	0.2295	-0.3419	0.2534	0.0
1	0.2295	1.0975	0.0	0.0	0.2295
2	-0.3419	0.0	0.8653	0.0	0.3419
3	0.2534	0.0	0.0	0.5272	0.2534
L	0.0	0.2295	0.3419	0.2534	0.0

(b)

	S	4	5	6	L
S	0.0	0.2534	-0.3419	0.2295	0.0
4	0.2534	-0.5272	0.0	0.0	0.2534
5	-0.3419	0.0	-0.8653	0.0	0.3419
6	0.2295	0.0	0.0	-1.0975	0.2295
L	0.0	0.2534	0.3419	0.2295	0.0

TABLE XI
ROTATION SEQUENCE FOR REDUCTION OF THE TRANSVERSAL MATRIX TO THE REQUESTED MATRIX WITH THE TOPOLOGY IN FIG. 11

Transform Number t	Element to be Annihilated		Pivot $[i,j]$	$\theta_r = -\tan^{-1}(cM_{kl}/M_{mn})$ k	l	m	n	c
M1								
1	$M1_{S3}$	In row 1	[2, 3]	S	3	S	2	-1
2	$M1_{S2}$	–	[1, 2]	S	2	S	1	-1
3	$M1_{24}$	In column 4	[2, 3]	2	4	3	4	+ 1
4	$M1_{13}$	In column 3	[1, 2]	1	3	2	3	+ 1
M2								
1	$M2_{S5}$	In row 1	[4, 5]	S	5	S	4	-1
2	$M2_{S6}$	–	[4, 6]	S	6	S	4	-1
3	$M2_{46}$	In row 2	[5, 6]	4	6	4	5	-1

It can be noted that the values of diagonal elements in the extracted matrix are also categorized into two groups, which are positive values and negative values, and corresponds to the resonant frequency of each resonator. Hence, the upper path governs the lower passband, and the trisection portion of the upper path provides a transmission zero on the lower stopband (i.e., -1.8 rad/s). Similarly, the lower path governs the upper passband and the trisection portion of the lower path generates a transmission zero on the upper stopband (i.e., 1.8 rad/s). By using such a dual-path coupling scheme, the transmission zeros on the upper and lower stopband can be generated by the trisection portion, while the additional transmission zero used to separate two passbands is generated by out-of-phase property of C_{N1} and C_{N2}.

The central frequencies of the two passbands in the practical design are 2.2 and 2.7 GHz, while the fractional bandwidth is 5% in each passband. For the practical implementation, a

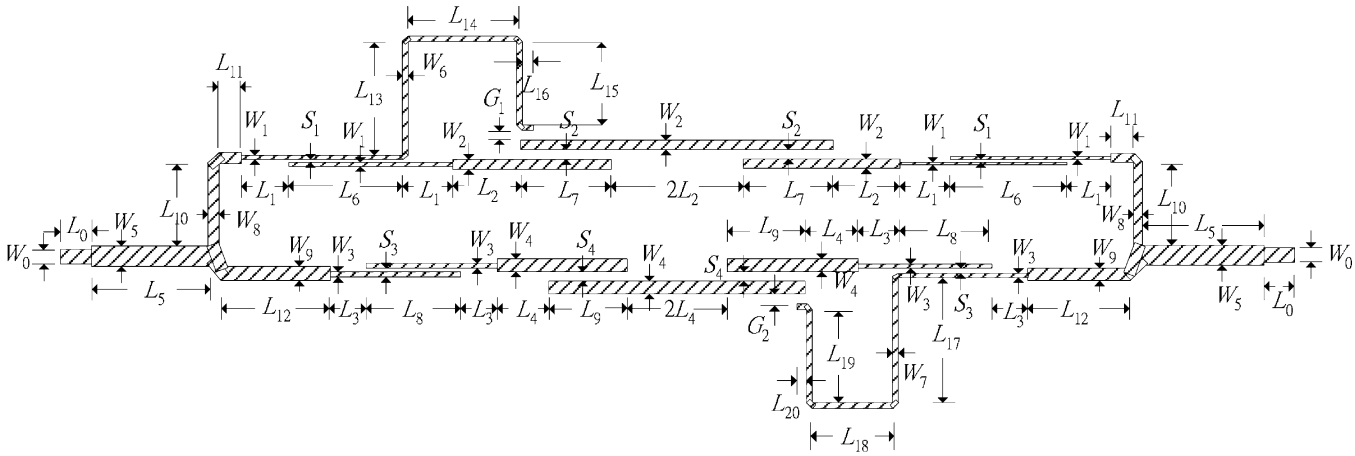

Fig. 12. Layout in example 2.

TABLE XII
COUPLING MATRIX FOR THE DUAL-BAND FILTER IN EXAMPLE 2 WITH THE DUAL-PATH COUPLING SCHEME SHOWN IN FIG. 11

	S	1	2	3	4	5	6	L
S	0.0	0.4739	-0.0958	0.0	0.4835	0.0	0.0	0.0
1	0.4739	0.9033	0.1880	0.0	0.0	0.0	0.0	0.0
2	-0.0958	0.1880	0.7619	0.2047	0.0	0.0	0.0	0.0
3	0.0	0.0	0.2047	0.8247	0.0	0.0	0.0	0.4835
4	0.4835	0.0	0.0	0.0	-0.8247	0.2047	0.0	0.0
5	0.0	0.0	0.0	0.0	0.2047	-0.7619	0.1880	0.0958
6	0.0	0.0	0.0	0.0	0.0	0.1880	-0.9033	0.4739
L	0.0	0.0	0.0	0.4835	0.0	0.0958	0.4739	0.0

TABLE XIII
DIMENSIONS IN EXAMPLE 2 (IN MILLIMETERS)

W_0	W_1	W_2	W_3	W_4	W_5	W_6	W_7
1.1180	0.2032	0.8636	0.4064	1.0160	1.1940	0.2286	0.2286
L_0	L_1	L_2	L_3	L_4	L_5	L_6	L_7
2.5400	3.9120	7.1120	2.9970	4.0130	9.2960	9.0420	7.1120
L_8	L_9	L_{10}	L_{11}	L_{12}	L_{13}	L_{14}	L_{15}
7.5180	6.0710	6.9090	1.6510	8.1030	9.3470	8.6870	6.9090
L_{16}	L_{17}	L_{18}	L_{19}	L_{20}	S_1	S_2	S_3
0.6850	10.5400	6.5530	8.0010	0.7112	0.2032	0.5080	0.2032
S_4	G_1	G_2					
0.5080	0.9144	1.0920					

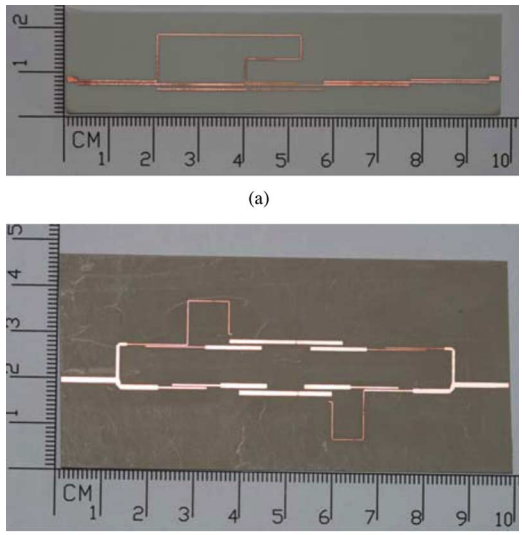

(a)

(b)

Fig. 13. Layout of the implemented filters in: (a) example 1 and (b) example 2.

0.635-mm-thick Rogers RT/Duroid 6010 substrate, with a relative dielectric constant 10.2 and a loss tangent of 0.0021, is used to implement such a dual-band filter. The practical dual-band microstrip parallel-coupled filter can also be implemented using the method in [16]. The layout of the dual-band microstrip filter is shown in Fig. 12 with the dimensions are listed in Table XIII.

V. RESULTS AND DISCUSSION

Fig. 13(a) and (b) shows the circuit photographs in example 1 and 2; Fig. 14(a) and (b) shows the individual simulated and measured performances and corresponding group delays. The EM simulator Sonnet is used to efficiently provide the simulated results [18]. In these two examples, the frequency shift between simulated and measured performances comes from the variation of the permittivity constant of the dielectric layer, so that it leads a difference between the practical design and simulation setup.

In exampe 1, Table VII shows that the element of cross coupling $M_{S,3}$ is 0.6590, which is even larger than the direct couple $M_{S,1}$ (0.5624) along the main path. Hence, the cross couple will be treated similarly as the direct coupled path between source and resonator 3. Such a strong cross-coupling strength $M_{S,3}$ contribute the separation of two passbands. In the practical design, the length of each coupled line section is initially set to be a quater-wave long at 2.5 GHz; it is then optimized by ADS optimization engine [19] to obtain the final practical length.

In the example 2, the transmission zeros within the stopbands are known to be governed by the trisection cross-coupling paths of coupling scheme $M_{S,2}$ and $M_{5,L}$ in Fig. 11. The corresponding element values are -0.0958 and 0.0958 in Table XII, which are smaller than the element value along the main path. This makes sense because the location of transmission zeros are far from the corresponding passbands. In Fig. 12, the lengths of the two coupling lines L_{16} (0.685 mm) and L_{20} (0.7112 mm) are obviously shorter than other coupled lines in the main path. The gaps G_1 and G_2 are also wider than the gaps of the main coupling path. Because of the dual-path schematic, a transmission zero to separate two passbands exists inherently.

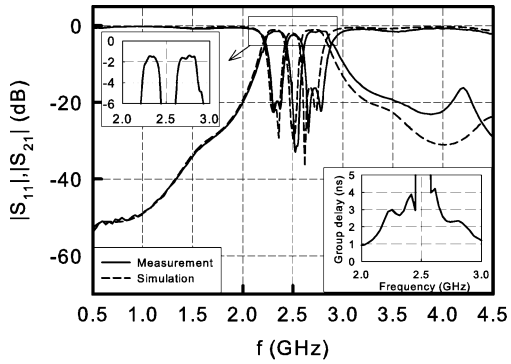

(a)

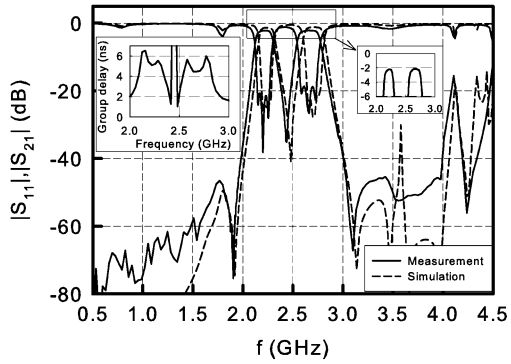

(b)

Fig. 14. Measured and simulated performances and group delay of the dual-band filter in: (a) example 1 and (b) example 2.

The dual-path coupling scheme also provides another advantage, which is the initial length of each coupled line that can be obtained at each resonant frequency due to each path governs one passband. After fine-tuning in ADS [19], the practical dimension will be obtained.

VI. Conclusion

The novel analytical method to synthesize a dual-band or a multiband filtering function has been successfully developed. Based on the synthesized composite filtering function, the transversal coupling matrix can be obtained. The transversal coupling matrix is then transformed to a specific coupling matrix, which makes it possible to implement a practical filter. The arbitrarily located transmission zeros and various bandwidth of each passband are available in this method. Furthermore, the single-path and dual-path dual-band coupling schemes are discussed to generate the transmission zeros for the dual-band filter design. By adding the additional quadruplet and trisection coupling scheme in the coupling scheme, the dual-band filter with finite transmission zeros is designed and implemented. The measured results have shown good agreement with simulated results. The newly dual-band transversal coupling matrix synthesis and proposed dual-band filter have shown properties of flexible responses, good performance, and quick design procedures.

Acknowledgment

The authors would like to thank one of the reviewers for very useful comments and detailed discussions.

References

[1] R. J. Cameron, "General coupling matrix synthesis methods for Chebyshev filtering functions," *IEEE Trans. Microw. Theory Tech.*, vol. 47, no. 4, pp. 433–442, Apr. 1999.

[2] R. J. Cameron, A. R. Harish, and C. J. Radcliffe, "Synthesis of advanced microwave filters without diagonal cross-couplings," *IEEE Trans. Microw. Theory Tech.*, vol. 50, no. 12, pp. 2862–2872, Dec. 2002.

[3] R. J. Cameron, "Advanced coupling matrix synthesis techniques for microwave filters," *IEEE Trans. Microw. Theory Tech.*, vol. 51, no. 1, pp. 1–10, Jan. 2003.

[4] R. J. Cameron, C. M. Kudsia, and R. R. Mansour, *Microwave Filters for Communication Systems: Fundamentals, Design, and Applications*. Hoboken, NJ: Wiley, 2007.

[5] P. Kozakowski, A. Lamecki, P. Sypek, and M. Mrozowski, "Eigenvalue approach to synthesis of prototype filters with source/load coupling," *IEEE Trans. Microw. Wireless Compon. Lett.*, vol. 15, no. 2, pp. 98–100, Feb. 2005.

[6] S. Amari, "Synthesis of cross-coupled resonator filters using an analytical gradient-based optimization technique," *IEEE Trans. Microw. Theory Tech.*, vol. 48, no. 9, pp. 1559–1564, Sep. 2000.

[7] A. G. Lamperez, "Analytical synthesis algorithm of dual-band filters with asymmetric pass bands and generalized topology," in *IEEE MTT-S Int. Microw. Symp. Dig.*, Honolulu, HI, Jun. 2007, pp. 909–912.

[8] G. Macchiarella and S. Tamiazzo, "Design techniques for dual-pass-band filters," *IEEE Trans. Microw. Theory Tech.*, vol. 53, no. 11, pp. 3265–3271, Nov. 2005.

[9] R. J. Cameron, M. Yu, and Y. Wang, "Direct-coupled microwave filters with single and dual stopbands," *IEEE Trans. Microw. Theory Tech.*, vol. 53, no. 11, pp. 3288–3297, Nov. 2005.

[10] S. Sun and L. Zhu, "Coupling dispersion of parallel-coupled microstrip lines for dual-band filters with controllable fractional pass bandwidths," in *IEEE MTT-S Int. Microw. Symp. Dig.*, Long Beach, CA, Jun. 2005, pp. 2195–2198.

[11] P. Lenoir, S. Bila, F. Seyfert, D. Baillargeat, and S. Verdeyme, "Synthesis and design of asymmetrical dual-band bandpass filters based on equivalent network simplification," *IEEE Trans. Microw. Theory Tech.*, vol. 54, no. 7, pp. 3090–3097, Jul. 2006.

[12] M. S. Wu, Y. Z. Chueh, J. C. Yeh, and S. G. Mao, "Synthesis of triple-band and quad-band bandpass filters using lumped-element coplanar waveguide resonators," *Prog. Electromagn. Res. B*, vol. 13, pp. 433–451, Jul. 2009.

[13] Y. Zhang, K. A. Zaki, J. A. Ruiz-Cruz, and A. E. Atia, "Analytical synthesis of generalized multi-band microwave filters," in *IEEE MTT-S Int. Microw. Symp. Dig.*, Honolulu, HI, 2007, pp. 1273–1276.

[14] M. Mokhtaari, J. Bornemann, K. Rambabu, and S. Amari, "Coupling-matrix design of dual and triple passband filters," *IEEE Trans. Microw. Theory Tech.*, vol. 54, no. 11, pp. 3940–3946, Nov. 2006.

[15] V. Lunot, F. Seyfert, S. Bila, and A. Nasser, "Certified computation of optimal multiband filtering functions," *IEEE Trans. Microw. Theory Tech.*, vol. 56, no. 1, pp. 105–112, Jan. 2008.

[16] J. C. Lu, C. K. Liao, and C. Y. Chang, "Microstrip parallel-coupled filters with cascade trisection and quadruplet responses," *IEEE Trans. Microw. Theory Tech.*, vol. 56, no. 9, pp. 2101–2110, Sep. 2008.

[17] G. Macchiarella and S. Tamiazzo, "Dual-band filters for base station multi-band combiners," in *IEEE MTT-S Int. Microw. Symp. Dig.*, Honolulu, HI, 2007, pp. 1289–1292.

[18] *"EM User's Manual,"* Sonnet Softw. Inc., Liverpool, NY, 2004.

[19] *"Advanced Design System (ADS),"* Agilent Technol., Santa Rosa, CA, 2003, ver. 2003C.

Yi-Ting Kuo was born in Tainan, Taiwan, on March 13, 1981. He received the B.S. degree in electrical engineering from the National Cheng Kung University, Tainan, Taiwan, in 2004, and is currently working toward the Ph.D. degree in communication engineering at the National Chiao-Tung University, Hsinchu, Taiwan.

His research interests include analysis and design of microwave filter, diplexer and multiplexer.

Jhe-Ching Lu was born in Kaohsiung, Taiwan, on May 18, 1982. He received the B.S. degree in electrical engineering from the National Sun Yat-Sen University, Kaohsiung, Taiwan, in 2004, the M.S. degree in communication engineering from the National Chiao-Tung University, Hsinchu, Taiwan, in 2006, and the Ph.D. degree in communication engineering from the National Chiao-Tung University, Hsinchu, Taiwan, in 2009.

He is currently a Principal Engineer with the Taiwan Semiconductor Manufacturing Company Ltd., Hsinchu, Taiwan. His research interests include the analysis and design optimization of microwave and millimeter-wave circuits, MOSFET modeling, and the deembedding technique.

Ching-Ku Liao was born in Taichung, Taiwan, on October 16, 1978. He received the B.S. degree in electrophysics and the M.S. and Ph.D. degrees in communication engineering from the National Chiao-Tung University, Hsinchu, Taiwan, in 2001, 2003, and 2007, respectively.

From 2006 to 2007, he was a Visiting Researcher with the University of Florida, Gainesville, sponsored by the National Science Council's Graduate Student Study Abroad Program. He is currently a Senior Engineer with the Gemtek Technology Company Ltd., Hsinchu, Taiwan. His research interests include the analysis and design of microwave and millimeter-wave circuits.

Dr. Liao is a member of Phi Tau Phi.

Chi-Yang Chang (S'88–M'95) was born in Taipei, Taiwan, on December 20, 1954. He received the B.S. degree in physics and M.S. degree in electrical engineering from the National Taiwan University, Taipei, Taiwan, in 1977 and 1982, respectively, and the Ph.D. degree in electrical engineering from The University of Texas at Austin, in 1990.

From 1979 to 1980, he was with the Department of Physics, National Taiwan University, as a Teaching Assistant. From 1982 to 1988, he was with the Chung-Shan Institute of Science and Technology (CSIST) as an Assistant Researcher, where he was in charge of development of microwave integrated circuits, microwave subsystems, and millimeter-wave waveguide E-plane circuits. From 1990 to 1995, he returned to CSIST as an Associate Researcher in charge of development of uniplanar circuits, ultra-broadband circuits, and millimeter-wave planar circuits. In 1995, he joined the faculty of the Department of Electrical Engineering, National Chiao-Tung University, Hsinchu, Taiwan, as an Associate Professor and became a Professor in 2002. His research interests include microwave and millimeter-wave passive and active circuit design, planar miniaturized filter design, and monolithic-microwave integrated-circuit design.